IOP Conf. Series: Materials Science and Engineering **381** (2018) 012021 doi:10.1088/1757-899X/381/1/012021

Thermodynamic Simulation of Components' Content in MoS_2 Hydrothermal Reaction System and Oxygen–Doped MoS_2 One-Step Hydrothermal Preparation Method

Guangtong Zhou[1], Hanjian Li[1], Xiangbin Zeng[2,a,*], Wenzhao Wang[2], Yishuo Hu[2], Shaoxiong Wu[2], Yang Zeng[2], Guanwei Chen[2], Zishen Guo[2], Yanhan Liu[2] and Haoran Zhang[2]

[1]China-EU Institute for Clean and Renewable Energy, Huazhong University of Science and Technology, Wuhan 430074, PR China
[2]School of Optical and Electronic information, HuaZhong University of Science and Technology Wuhan, 430074 PR China
Email: [a]eexbzeng@163.com

Abstract. Binary nanocomposites of Oxygen-doped molybdenum disulfide was prepared through one-step hydrothermal method. Different effects of initial addition amount of sulfur, hydrazine hydrate and molybdenum oxide on the reaction products were investigated by HCS Chemistry. The direction and process of the hydrothermal reaction were determined by the principle of lowest Gibbs free enthalpy and the components' content in the reaction system were simulated. Scanning Electron Microscopy (SEM), Raman Spectroscopy (Raman) and X-ray (XRD) was used to characterize the experimental results.

1. Introduction

Transition metal disulfide MS_2 (M = Mo, W, Nb, Ta, Ti, Re) is characterized by its unique electrical, magnetic, optical and thermal properties in capacitors, catalysis, lithium batteries, hydrogen storage and evolution, Semiconductor and other fields [1-5]. Among them, molybdenum disulfide (MoS_2) is widely used in many fields for its unique atomic structure. MoS_2 has a hexagonal crystal lamellar structure, similar to graphene, layers are bounded by van der Waals force, while the layer consisting S-Mo-S three atoms is covalently bonded to form a regular hexagonal structure. Monolayer MoS_2 (about 0.7 nm) is a 1.8eV [6, 7] direct bandgap material. Compared with the zero bandgap graphene, molybdenum disulfide has a brighter application prospect in optoelectronic devices, due to adjustable band gap [8-10]; Compared to the three-dimensional bulk structure silicon, molybdenum disulfide can be used to fabricate semiconductors or smaller but more efficient electronic chips, due to the nanoscale two-dimensional film structure [11-16].

In recent years, regulating the carrier type and concentration in the channel of MoS_2 through controllable doping, in order to improve the device performance and realize the functional coordination and device integration, has become a new hot spot. Current doping methods can be divided into three kinds: (1) Surface charge transfer [17, 18]: Deposit or adsorb withdrawing/gain electron atoms, small molecules or polymers by the surface charge transfer effect; (2) Element substitution [19, 20]: During or after the growth process, replace molybdenum or sulfur atoms with other atoms; (3) Intercalation [21, 22]: Insert atoms, molecules or ions between layers. More specific, elemental substitution methods can be divided into molybdenum substitution and sulfur substitution. For sulfur substitution methods, Duan [23] et al. used Se to replace part of S and obtained $MoS_{2x}Se_{2\,(1-x)}$

with band gap differed from 1.85eV to 1.55eV through CVD method, Qin [24] et al. prepared N-doped MoS_2 with better catalytic hydrogen evolution capacity through sol-gel method. LAI GuoHong [26] et al. reported that oxygen substitution can effectively increase the light absorption bandwidth, enhance the light absorption properties in UV-Vis light bands, and improve the photoelectric properties of monolayer MoS_2, through first principle calculations. However, the controlled oxygen doping method has not been reported till now.

In this paper, the components' content in the reaction system was simulated with HCS Chemistry, the effects of temperature and reactant compositions were analyzed by thermodynamic methods. Finally, we proposed an one-step hydrothermal preparation method of oxygen-doped MoS_2.(HCS Chemistry is a software developed by the United States Outo-kumpu research center for the chemical reaction balance calculation of the integrated thermodynamic, and it is the world's most widely used chemical thermodynamics calculation software.)

2. Thermodynamic analysis of components' content in MoS_2 hydrothermal reaction system

The Gibbs free energy is a thermodynamic function used to determine the direction of the reaction process. In this paper, we used Molybdenum oxide (MoO_3), hydrazine hydrate (N_2H_4) and sulfur (S) as raw materials and deionized water as solvent. We used the parameters of formulas (1) to (6) and Table 1 to calculate and analyze the possible products of hydrothermal reaction. The minimum Gibbs free energy was used to judge the reaction process of the system.

Hydrothermal reaction can be considered to be at a state with constant temperature, constant pressure and non-volumetric zero. In the formula (1), the C$p.m$ is the molar heat capacity at constant pressure, varies with the temperature, while A, B, C, D is the corresponding coefficient. In Formula (2), the $\Delta_r C_{p\cdot m}$ is the reaction molar heat capacity difference, which can be calculated by summing the product of the reaction stoichiometric coefficients ν and all the substance's molar heat capacity involved in the reaction. Similarly, in formula (3) and (4), the reaction enthalpy $\Delta_r H_m^\theta$ and the reaction entropy $\Delta_r S_m^\theta$ can be calculated. Formula (5) and (6) are used to convert the reaction enthalpy and entropy into those of the hydrothermal reaction temperature. The Gibbs free energy of the reaction can be calculated by the formula (7).

$$C_{p\cdot m} = A + BT + CT^3 + \mathrm{D}T^4 \tag{1}$$

$$\Delta_r C_{p\cdot m} = \sum \nu_B C_{p.m}(B) \tag{2}$$

$$\Delta_r H_m^\theta = \sum \nu_B H_m^\theta(B) \tag{3}$$

$$\Delta_r S_m^\theta = \sum \nu_B S_m^\theta(B) \tag{4}$$

$$\Delta_r H_m^\theta(T) = \sum \Delta_r H_m^\theta(298.15K) + \int_{298.15K}^{T} \Delta_r C_{p\cdot m} dT \tag{5}$$

$$\Delta_r S_m^\theta(T) = \sum \Delta_r S_m^\theta(298.15K) + \int_{298.15K}^{T} \frac{\Delta_r C_{p\cdot m}}{T} dT \tag{6}$$

$$\Delta_r G_m^\theta(T) = \Delta_r H_m^\theta(T) - T\Delta_r S_m^\theta(T) \tag{7}$$

Theoretically, the reaction equilibrium of MoO_3 completely generated to MoS_2 by hydrothermal reaction is shown as follows:

$$MoO_3 + 6N_2H_4(g) + 2S = MoS_2 + 3N_2(g) + 3H_2O(g) + 6NH_3(g) \tag{8}$$

According to formula (8), we firstly set the initial addition amount of MoO_3 as the reaction coefficient, namely 1mol. The reaction temperature was set at 200 ℃ (reported hydrothermal reaction temperature),

the pressure was set as 30bar (standard hydrothermal reaction vessel pressure limit) and the initial amount of deionized water was 10mol (saturated vapor pressure with excess water content), to explore the change rules of reaction products with different initial addition amount of S, N_2H_4 and MoO_3 respectively.

2.1. Effects of initial addition amount of S and N_2H_4 on hydrothermal products

Sulfur, as a sulfur source for the preparation of MoS_2, will only be reduced to S^{2-} in hydrazine hydrate reductive atmosphere theoretically. However, the amount of sulfur added has a great influence on the whole reaction process and the products practically, on the one hand S^{2-} has many compounds, on the other hand there is a competitive relationship between the presence of S as the oxidant and Mo^{6+}, so it is very important to study the effects of S.

According to formula (8), we set MoO_3 1mol and N_2H_4 6mol as the initial addition amount, the amount of sulfur was increased from 0mol to excess to simulate the components' content in the hydrothermal reactor. The simulation results are shown in Figure 1.

When sulfur is 0mol, the reaction is:

$$3MoO_3 + 18N_2H_4\,(g) = 3MoO_2 + 7N2(g) + 3H2O\,(g) + 22NH3(g) \quad (9)$$

Here Mo^{6+} is reduced to Mo^{4+}, in the form of MoO_2, excess N_2H_4 will conduct its own disproportionation reaction:

$$3N_2H_4(g) = N_2(g) + 4NH_3(g) \quad (10)$$

With the increasing amount of S, Mo^{6+} is still reduced to $Mo4^{+}$, while all S is reduced to S^{2-}, the product is a mixture of MoO_2 and MoS_2, until the addition of S reached to 2mol. The reaction occurred at that time is just as it shows in formula (8), all Mo is present in the form of MoS_2.

The reaction that occurs in the next stage is based on the reaction of formula (8), only adds the reduction of S by N_2H_4:

$$N_2H_4(g) + 2S = N_2(g) + 2H_2S\,(g) \quad (11)$$

MoS_2 maintains to be the vast majority of Mo existence in the reaction system until the S addition amount reaches 10mol. During the process, there is a competition between oxidizing agent: when S increased to 7 ~ 8mol, although oxidizability of Mo^{6+} is stronger than S, but the large presence of S will gradually dominate the competition of reducing agent, so part of the Mo^{6+} is not been reduced and forms as MoS_3.

When the addition amount of S reaches 12mol, MoS_3 will become the only form of molybdenum in the system. The sulfur element will exhaust all the reduction capacity of hydrazine hydrate, and the final reaction is:

$$MoO_3+6N_2H_4(g)+12S=6N_2(g)+3H_2O(g)+MoS_3+9H_2S(g) \quad (12)$$

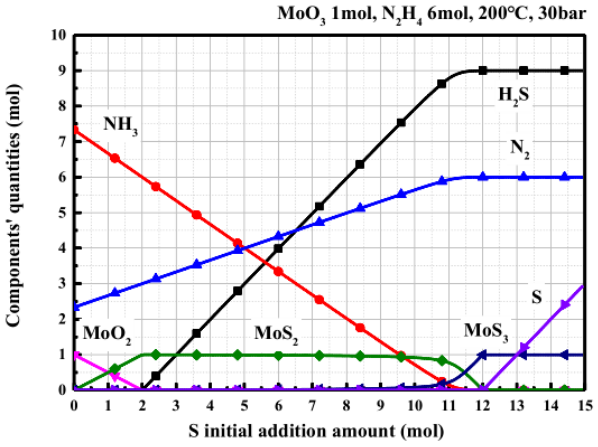

Figure 1. Change of the component content with different amount of S initial addition.

When S is extensively added, the Mo in MoS_3 is not in the same valence state as Mo in MoS_2. At the same time, MoS_3 is not stable and we haven't find any mature application report, so we have control the addition of S accurately. When S is slightly added, a mixture of MoS_2 and MoO_2 is formed, which is likely to form oxygen-doped MoS_2, but the reducing agent N_2H_4 plays an extremely important role.

In order to analyze the effect of N_2H_4, we set the initial addition amount of MoO_3 and S as 1mol and 2mol.

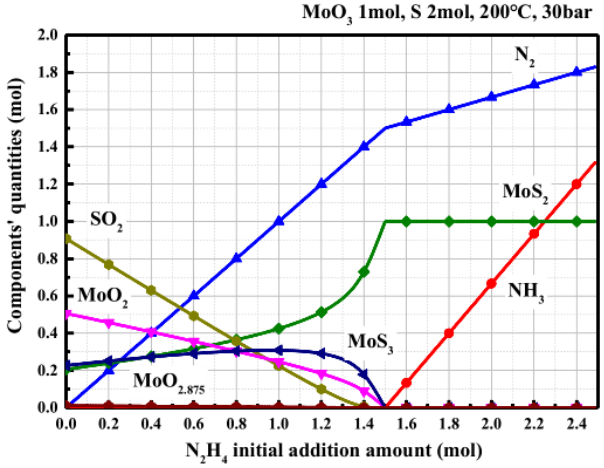

Figure 2. Components' quantities versus N_2H_4 initial addition amount in hydrothermal reaction system at 200 ℃ 300bar, with 1mol MoO_3 and 2mol S initially added.

Figure 2 shows the simulation results. It is not difficult to find that N_2H_4 functioning as reducing agent has an extremely important effect on the composition of the reaction products. When N_2H_4 is added not that much (less than 1.5mol), the reaction is quite complex. When the amount of hydrazine hydrate is insufficient, MoO_3 is partly reduced to MoO_X (X= 2~3), and partly forms as MoS_2 and MoS_3; S functions as a reducing agent and is partly oxidized to SO_2. With the increase of N_2H_4, the reducing agent S is gradually replaced, and the amount of SO_2 decreases rapidly; The morphology of Mo tends to be uniform, high valence state Mo is gradually reduced to lower valence state Mo. However, during this period, the proportion of MoS_3 is increased first and then down. It is probably because: although the oxidizability of Mo^{6+} is higher than S, but it is much lower than SO_2, N_2H_4 will try to avoid the oxidation of S, so S will be reduced to S^{2-} as much as possible; However, after the exhaustion of N_2H_4, the remaining S will still be oxidized by Mo^{6+}, but the amount of this part S is very small, so there is more Mo^{6+} in the system in the form of MoS_3 than when there is no N_2H_4 existing, and that is why MoS_3 will show an increasing trend; Subsequently, due to the further increase of N_2H_4, more Mo^{6+} will be reduced to Mo^{4+}, so the amount of MoS_3 gradually reduces.

In general, Mo^{6+} and S are in a dynamic competitive relationship when hydrazine hydrate is slightly added. Even though the dominant position of the oxidant is occupied at the beginning, the reduction proportion will also be a disadvantage in the competition of reducing agent in the later stage of the reaction.

When the initial addition amount of N_2H_4 reaches 1.5 mol, Mo and S in the system are reduced to Mo^{4+} and S^{2-}, the final molybdenum will all be in the form of MoS_2, the reaction is:

$$2MoO_3 + 3N_2H_4(g) + 4S = 2MoS_2 + 3N_2(g) + 6H_2O(g) \quad (13)$$

While the amount of hydrazine hydrate is further increased, the form of molybdenum and sulfur in the system does not change, the excess N_2H_4 will occur in the disproportionation reaction, as shown in equation (10).

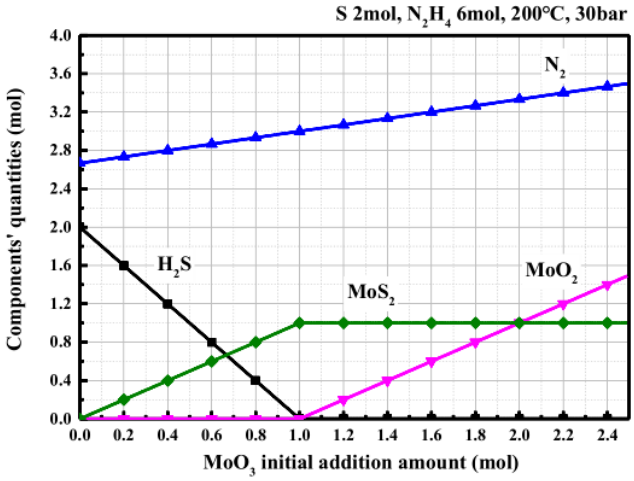

Figure 3. Change of the component content with different amount of MoO_3 initial addition.

Finally, we obtain the result that when the initial addition amount MoO_3: N_2H_4: S is 1:1.5:2, the only two reaction products are MoS_2 and N_2, theoretically; Excess hydrazine hydrate is beneficial to protect MoS_2 as the sole product; Appropriate reduction of S addition may form a mixture of MoS_2 and MoO_2, that is oxygen-doped MoS_2.

In this case, we set the initial addition amount of S to 2mol and the initial addition amount of N_2H_4 is 20mol, considering hydrazine hydrate could be easily decomposed. With the addition amount of MoO_3 is gradually increased from 0mol to 2.5mol, the material composition of the system is simulated to verify the preparation method of oxygen doped MoS_2.

2.2. Effect of Initial addition of molybdenum on reaction products

As is shown in Figure 3 (NH_3 is omitted for the large emission amount), a sufficient addition amount of N_2H_4 can effectively limit the form of Mo, all the Mo in the system is Mo^{4+}. When MoO_3 is added in a small amount, it is all in the form of MoS_2; When it is initially added in an amount of 1mol or more, extra MoO_3 will only generates MoO_2 in the reaction system, without any other form of Mo.

The result further confirms previous simulation results in section 1.2. Depending on the results, we propose a one-step hydrothermal method for the preparation of oxygen doped MoS_2 by controlling MoO_3, N_2H_4 and S initial addition amount: S added slightly less than 2 times the initial addition amount of MoO_3 and keeping N_2H_4 excessive. In this way, oxygen doped MoS_2 was prepared by one-step hydrothermal method without other post processing.

In order to verify the results of simulation, MoO_3, N_2H_4 and S initial addition ratio of the amount of material is 1:20:1.9 was prepared, and select MoO_3, N_2H_4 and S initial addition ratio 1:20:2 as a reference, the oxygen doped MoS_2 prepared by one step hydrothermal method was characterized by modern analytical methods.

3. Experiment

3.1. Experimental materials and methods

3.1.1. Preparation of MoO_3. 0.75 g of $(NH_4)_6Mo_7O_{24}$ (Aladdin, AR, the ACS, 81-83% AS MoO_3) is dispersed in 10ml deionized water and stirred to dissolved, moderate amount of dilute nitric acid is added and thoroughly mixed, then the mixed solution is transferred to a 25 ml polytetrafluoroethylene liner and wrapped in the stainless steel hydrothermal reactor. The mixture was heated at 180 ℃ for 24 h in a blast oven and cooled down under nature conditions, then treated with deionized water and anhydrous Ethanol, washed and centrifuged several times, and finally dried in a vacuum oven at 60 ℃ for 4 h, stored for further using.

3.1.2. Preparation of MoS_2 and the Oxygen Doped MoS_2. 0.68 g MoO_3 prepared by the above method (0.75 g for the oxygen-doped MoS_2) mixed with 0.3g S (Medicines, AR, the AR, 99.9%) were dispersed in 5ml hydrazine hydrate (Ji Ning Hongming chemistry, AR, the AR, 80%), then the fully mixed solution was transferred to a 25ml polytetrafluoroethylene liner wrapped in stainless steel hydrothermal reactor. Appropriate amount of deionized water was added until the mixed solution reached 60% of the total volume of the liner, heated at 200℃ for 24 h, and then cooled to room temperature.

3.1.3. Characterize the Morphology, Composition and Structure of the Material. Use field emission scanning electron microscope (FE-SEM, HITACHI S-4800, 5.0 kV), laser confocal Raman spectroscopy (Horiba JobinYvon LabRAM HR800 532 nm 200-1100), X-ray diffractometer (XRD, PANalytical PW3040 / 60, voltage 40 kV, current 40 mA, Cu Kα radiation (λ= 1.5406), 2θ=10°~ 80°) to characterize the morphology, composition and crystal structure of samples.

3.2. Experimental results

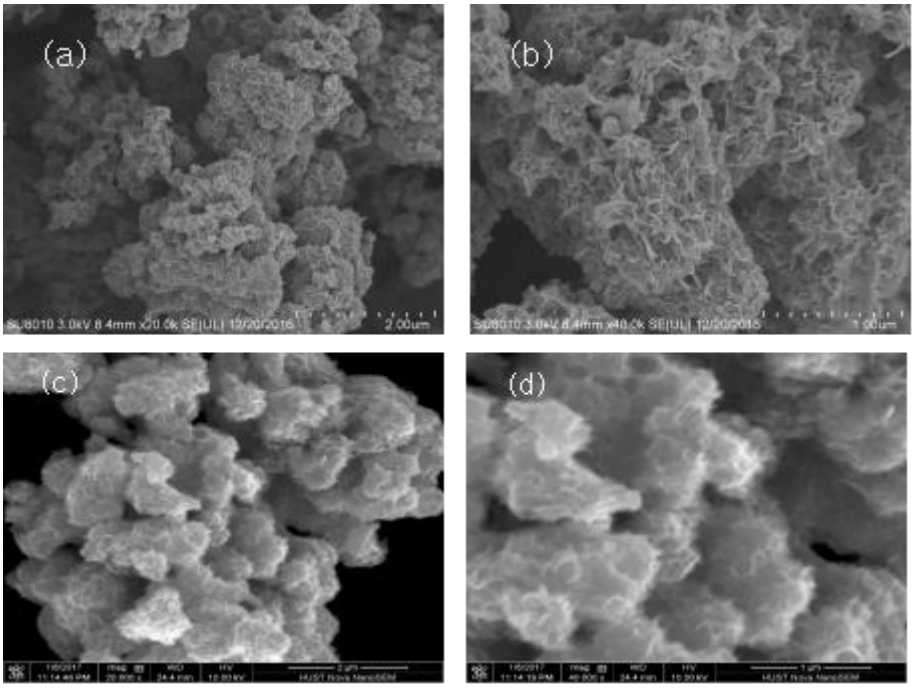

Figure 4. SEM of MoS_2 and oxygen doped MoS_2 prepared by hydrothermal method. ((a) MoS_2 20k (b) MoS_2 40k (c) Oxygen doped MoS_2 20k (d) Oxygen doped MoS_2 40k)

Figure 4 shows prepared MoS_2 and the oxygen-doped MoS_2 SEM photographs by hydrothermal method. It is not difficult to find that whether MoS_2 or oxygen-doped MoS_2, is composed of many flakes clusters, and the thickness of these flakes is of nanometer level. The thickness of monolayer MoS_2 is about 0.8nm, hydrothermal method prepared MoS_2 is possible to form a two-layer, three-layer or multi-layer laminated structure, which is consistent with the observed SEM results.

Comparing the MoS_2 and the oxygen-doped MoS_2 SEM images, it can be found that the oxygen-doped MoS_2 has a larger agglomerate, the average cluster diameter is 0.5μm, and the size of the extended sheets are relatively short, which is very similar to the structure of MoO_2 nanoparticles in reports[25]. In MoS_2, the average cluster diameter is about 0.1μm, the sheet is more intensive with some flaky folds on the surface, which indicates that MoS_2 is epitaxial grown during the hydrothermal reaction; MoO_3 is first reduced to MoO_2, and then grow up to form MoS_2 flakes on the MoO_2 surface. When preparing oxygen-doped MoS_2, because of the overdose of the MoO_3, the vulcanization reaction of MoO_2 is not complete, resulting in larger clusters and shorter elongation.

Figure 5 is MoS_2 and oxygen-doped MoS_2 Raman spectures. Figure 5(a) shows that the out-of-plane vibration mode A_{1g} peak of MoS_2 located at 403cm^{-1}, while the in-plane vibration mode E_{2g} located at 382cm^{-1}, consistent with the data in the Lloyd Twaites database. Obviously, hydrothermal method can be used to prepare MoS_2 with high purity.

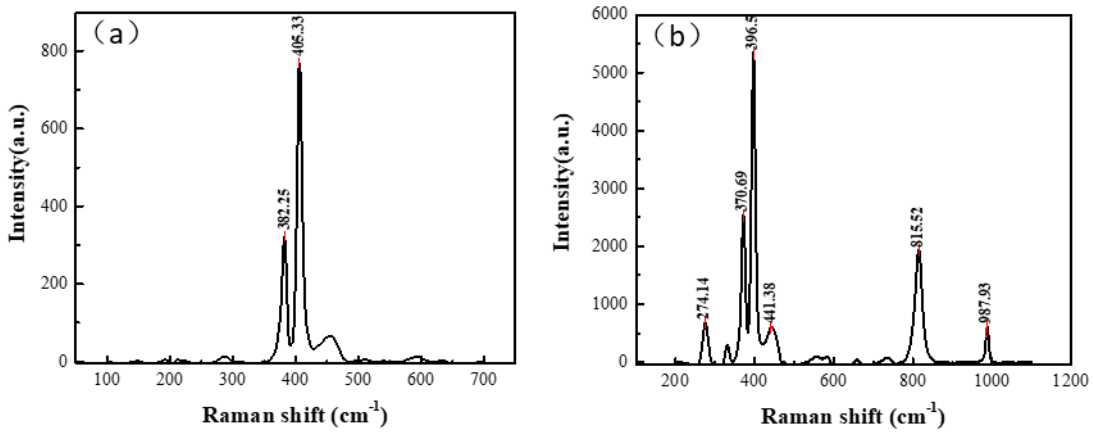

Figure 5. Raman spectra of MoS_2 and oxygen doped MoS_2 prepared by hydrothermal method. ((a) MoS_2 (b) Oxygen doped MoS_2)

Figure 5(b) shows that the out-of- plane vibration mode A_{1g} peak of MoS_2 located at 396 cm^{-1}, in-plane vibration mode E_{2g} located at 370 cm^{-1}, presenting a very obvious redshift. It can be explained by the dielectric limit effect: the increasing Coulomb force between charged particles increases the binding energy and the vibrator intensity between the electrons and holes, which weak the quantum confinement effect and the space confinement, energy change caused by surface effect is greater than that caused by the spatial effect, so that the band gap can be reduced, which leads to spectral redshift. These result is consistent with the simulation of Lai Guohong[27] that the bandgap of MoS_2 reduce to 1.4eV from 1.8eV after oxygen doping.

The two absorption peaks of wave number 815cm^{-1} and 987cm^{-1} in Figure 5(b) belong to MoO_3, probably because the stabilization of MoO_3 is better than MoO_2. Insufficient vacuum in the vacuum drying process resulted in the oxidation of MoO_2, or slow oxidation of MoO_2 during storage resulting in the formation of MoO_3.

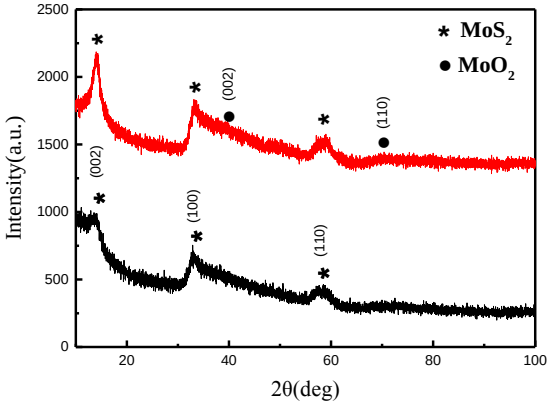

Figure 6. XRD pattern of MoS_2 and oxygen doped MoS_2 prepared by hydrothermal method. ((a) MoS_2 (b) Oxygen doped MoS_2)

Figure 6 shows the XRD patterns of MoS_2 and oxygen doped MoS_2. The diffraction peaks of both MoS_2 and oxygen doped MoO_2 are weak, corresponding to low crystallization degree. The XRD

patterns of MoS_2 are consistent with the standard card (JCPDS 337-1492), which indicates that MoS_2 with hexagonal system was obtained by hydrothermal method. In the XRD pattern of oxygen-doped MoS_2, we can find the two weak peaks near 40 ° and 65 °, which are belonging to <002> and <110> crystallographic orientation of MoO_2 (JCPDS 76-1003).

Through the analysis of experimental results, we can conclude that the feasibility of preparation oxygen-doped MoS_2 by one Step hydrothermal method.

4. Conclusion

HCS Chemistry was used to simulate the effect of sulfur (S) and hydrazine hydrate (N_2H_4) initial addition amount on the hydrothermal products, we found that: with an excess of hydrazine hydrate and slightly less than 2:1 initial addition amount of S:MoO_3, we can get the mixture of MoO_2 and MoS_2. The initial addition amount of molybdenum oxide (MoO_3) is also simulated to verify the results. In turn, we present an one-step hydrothermal preparation method of oxygen-doped MoS_2. By comparing the experimental results of MoS_2 and oxygen doped MoS_2 prepared by hydrothermal method, we verified the feasibility of one-step preparation method and finally we got oxygen-doped MoS_2 with nanostructure clusters.

5. References

[1] Ma, G., Peng, H., Mu, J., Huang, H., Zhou, X., & Lei, Z. (2013). In situ intercalative polymerization of pyrrole in graphene analogue of MoS_2 as advanced electrode material in supercapacitor. Journal of Power Sources, 229, 72-78.

[2] Huang, K. J., Wang, L., Liu, Y. J., Wang, H. B., Liu, Y. M., & Wang, L. L. (2013). Synthesis of polyaniline/2-dimensional graphene analog MoS_2 composites for high-performance supercapacitor. Electrochemical Acta, 109, 587-594.

[3] Zhou, W., Yin, Z., Du, Y., Huang, X., Zeng, Z., Fan, Z., ... & Zhang, H. (2013). Synthesis of few‐layer MoS_2 nanosheet- coated TiO_2 nanobelt heterostructures for enhanced photocatalytic activities. Small, 9(1), 140-147.

[4] Yin, Z., Chen, B., Bosman, M., Cao, X., Chen, J., Zheng, B., & Zhang, H. (2014). Au Nanoparticle‐Modified MoS_2 Nanosheet‐Based Photo electrochemical Cells for Water Splitting. Small, 10(17), 3537- 3543.

[5] Su, D., Dou, S., & Wang, G. (2014). WS2@ graphene nanocomposites as anode materials for Na-ion batteries with enhanced electrochemical performances. Chemical Communications, 50(32), 4192- 4195.

[6] Splendiani, A., Sun, L., Zhang, Y., Li, T., Kim, J., Chim, C. Y., ... & Wang, F. (2010). Emerging photoluminescence in monolayer MoS_2. Nano letters, 10(4), 1271-1275.

[7] Mak, K. F., Lee, C., Hone, J., Shan, J., & Heinz, T. F. (2010). Atomically thin MoS_2: a new direct-gap semiconductor. Physical Review Letters, 105(13), 136805.

[8] [8] Dresselhaus, M. S., Chen, G., Tang, M. Y., Yang, R. G., Lee, H., Wang, D. Z., ... & Gogna, P. (2007). New Directions for Low- Dimensional Thermoelectric Materials. Advanced Materials, 19(8), 1043-1053.

[9] Soon, J. M., & Loh, K. P. (2007). Electrochemical double-layer capacitance of MoS_2 nanowall films. Electrochemical and Solid-State Letters, 10(11), A250-A254.

[10] Tanaka, H., Okumiya, T., Ueda, S. K., Taketani, Y., & Murakami, M. (2009). Preparation of nanosheet by exfoliation of layered iron phenyl phosphate under ultrasonic irradiation. Materials Research Bulletin, 44(2), 328-333.

[11] Radisavljevic, B., Radenovic, A., Brivio, J., Giacometti, I. V., & Kis, A. (2011). Single-layer MoS_2 transistors. Nature nanotechnology, 6(3), 147-150.

[12] Bromley, R. A., Murray, R. B., & Yoffe, A. D. (1972). The band structures of some transition metal dichalcogenides. III. Group VIA: trigonal prism materials. Journal of Physics C: Solid State Physics, 5(7), 759.

[13] Mattheiss, L. F. (1973). Band structures of transition-metal-dichalcogenide layer compounds. Physical Review B, 8(8), 3719.

[14] Coehoorn, R., Haas, C., Dijkstra, J., Flipse, C. J. F., De Groot, R. A., & Wold, A. (1987). Electronic structure of $MoSe_2$, MoS_2, and WSe_2. I. Band-structure calculations and photoelectron spectroscopy. Physical Review B, 35(12), 6195.
[15] Böker, T., Severin, R., Müller, A., Janowitz, C., Manzke, R., Voß, D., ... & Pollmann, J. (2001). Band structure of MoS_2, $MoSe_2$, and α− $MoTe_2$: Angle-resolved photoelectron spectroscopy and ab initio calculations. Physical Review B, 64(23), 235305.
[16] Balendhran, S., Ou, J. Z., Bhaskaran, M., Sriram, S., Ippolito, S., Vasic, Z., ... & Kalantar-Zadeh, K. (2012). Atomically thin layers of MoS_2 via a two steps thermal evaporation–exfoliation method. Nanoscale, 4(2), 461-466.
[17] XING, L., & JIAO, L. Y. (2016). Recent Advances in the Chemical Doping of Two-Dimensional Molybdenum Disulfide. Acta Phys Chim Sin, 32(9), 2133-2145.
[18] XING, L., & JIAO, L. Y. (2016). Recent Advances in the Chemical Doping of Two-Dimensional Molybdenum Disulfide. Acta Phys Chim Sin, 32(9), 2133-2145.
[19] Gong, Y., Liu, Z., Lupini, A. R., Shi, G., Lin, J., Najmaei, S., ... & Terrones, H. (2013). Band gap engineering and layer-by-layer mapping of selenium-doped molybdenum disulfide. Nano letters, 14(2), 442-449.
[20] Yang, L., Fu, Q., Wang, W., Huang, J., Huang, J., Zhang, J., & Xiang, B. (2015). Large-area synthesis of monolayered MoS_2 (1− x) Se_2x with a tunable band gap and its enhanced electrochemical catalytic activity. Nanoscale, 7(23), 10490-10497.
[21] Lukowski, M. A., Daniel, A. S., Meng, F., Forticaux, A., Li, L., & Jin, S. (2013). Enhanced hydrogen evolution catalysis from chemically exfoliated metallic MoS_2 nanosheets. Journal of the American Chemical Society, 135(28), 10274-10277.
[22] Xiong, F., Wang, H., Liu, X., Sun, J., Brongersma, M., Pop, E., & Cui, Y. (2015). Li intercalation in MoS_2: in situ observation of its dynamics and tuning optical and electrical properties. Nano letters, 15(10), 6777-6784.
[23] Li, H., Duan, X., Wu, X., Zhuang, X., Zhou, H., Zhang, Q., ... & Ma, L. (2014). Growth of Alloy MoS_{2x} $Se_{2\ (1–x)}$ Nanosheets with Fully Tunable Chemical Compositions and Optical Properties. Journal of the American Chemical Society, 136(10), 3756-3759.
[24] Zhou, W., Hou, D., Sang, Y., Yao, S., Zhou, J., Li, G., ... & Chen, S. (2014). MoO_2 nanobelts @ nitrogen self-doped MoS_2 nanosheets as effective electrocatalysts for hydrogen evolution reaction. Journal of Materials Chemistry A, 2(29), 11358-11364.
[25] Wu, J., Lu, D., Fang, Z., Zhang, R., Zhu, Y., Zhu, R., & Yi, T. (2016). Hydrothermal Synthesis and Electrochemical Performance of MoO_2 as Anode Materials for Lithium-ion Batteries. Nonferrous Metals Engineering, 6(1), 27-30.
[26] Lai, G., Yu, Z., Zhang, C., & Liao, H. (2015). Electronic Structure and Photoelectric Properties of O-and Se-doped Single-layer MoS_2. Materials Review, 29 (18), 000152-159.
[27] Dieterle, M., & Mestl, G. (2002). Raman spectroscopy of molybdenum oxides Part II. Resonance Raman spectroscopic characterization of the molybdenum oxides Mo_4O_{11} and MoO_2. Physical Chemistry Chemical Physics, 4(5), 822-826.